

Phase Noise and Carrier Frequency Offset in OFDM systems: Joint Estimation and Hybrid Cramér-Rao Lower Bound

Omar Hazim Salim, Ali A Nasir, Hani Mehrpouyan, and Wei Xiang,

email: OmarHazim.Salim@usq.edu.au, ali.nasir@anu.edu.au, Hani.mehr@ieee.org, wei.xiang@usq.edu.au.

Abstract—In this paper, a new iterative pilot-aided algorithm based on expectation conditional maximization (ECM) for joint estimation of Wiener phase noise (PHN) and carrier frequency offset (CFO) in orthogonal frequency division multiplexing (OFDM) systems is proposed. Next, a new expression for the hybrid Cramér-Rao lower bound (HCRB) for joint estimation of PHN and CFO in OFDM systems is derived. Numerical results show that the proposed estimator outperforms existing algorithms in terms of mean square error while performing close to the derived HCRB at moderate PHN variances. Moreover, the proposed estimator is found to be computationally more efficient than existing algorithms since it jointly estimates PHN and CFO in a few iterations.

I. INTRODUCTION

Orthogonal frequency division multiplexing (OFDM) is a powerful multicarrier modulation technique that can increase the bandwidth efficiency of wireless systems [1]. However, OFDM systems are very sensitive to imperfect synchronization, where phase noise (PHN) and carrier frequency offset (CFO), caused by instable oscillators and Doppler shift, result in a common phase error (CPE) and inter-carrier interference (ICI) at the receiver. Both of these factors can lead to the degradation of system performance [2]. Therefore, these imperfections need to be accurately estimated to mitigate the resulting CPE and ICI.

Many CFO and PHN estimators are proposed for mitigating the effects of CPE and ICI, e.g., [3] and [4]. However, the estimation approach in [3] is based on a small angle approximation that adversely affects estimation performance. The approach in [3] is also computationally very complexity because it requires large matrix inversions [5]. Most recently, the authors in [4] proposed a new PHN and CFO estimation based on the expectation-maximization approach. Even though the estimator in [4] can track the PHN parameters, its performance is only verified at signal-to-noise ratio (SNR) of 10 dB, it requires a large number of iterations, and it is not in closed-form. More importantly, both [3] and [4] do not provide the Cramér-Rao lower bound (HCRB) for joint estimation of PHN and CFO in OFDM systems.

The HCRB is used in many studies to analyze the accuracy of joint estimation of deterministic and random parameters [5]–[9]. For example, the Bayesian Cramér-Rao lower bound

Omar Hazim Salim and Wei Xiang are with the Faculty of Engineering and Surveying, University of Southern Queensland, Australia, Ali A Nasir is with the Research School of Information Sciences and Engineering, the Australian National University, Australia, and Hani Mehrpouyan is with the Department of Electrical and Computer Engineering and Computer Science, California State University, Bakersfield, USA.

for Brownian PHN estimation while ignoring the effect of CFO is derived in [6], [7], [9], [10]. Recently, the HCRB for joint CFO and channel estimation in OFDM systems is derived in [5], [8]. However, the HCRB for joint PHN and CFO estimation in OFDM systems is not studied to date.

In this paper, we present a new approach for carrier recovery in OFDM systems. As such, the contributions of this paper can be summarized as follows:

- A new expression for the HCRB for joint estimation of the PHN and CFO in OFDM systems is derived.
- A new iterative pilot-aided algorithm based on the expectation conditional maximization (ECM) for joint estimation of PHN and CFO in OFDM systems is proposed.
- Simulations are carried out to investigate the performance of the proposed estimator. These simulation results demonstrate that the proposed estimator's performance is close to the HCRB for moderate PHN variances while outperforming the algorithm in [3] at medium to high SNRs

The rest of this paper is organized as follows: Section II describes the system model, the scenario under consideration, and the assumptions in this work. Section III derives an expression for the HCRB for PHN and CFO estimation in OFDM systems. In Section IV, the proposed estimator is derived while in Section V simulation results that investigate the performance of the proposed estimator are presented. Section VI concludes the paper.

Notations: Superscripts $(\cdot)^*$, $(\cdot)^H$, and $(\cdot)^T$ denote the conjugate, the conjugate transpose, and the transpose operators, respectively. Bold face small letters, e.g., \mathbf{x} , are used for vectors, bold face capital alphabets, e.g., \mathbf{X} , are used for matrices, and $[\mathbf{X}]_{x,y}$ represents the entry in row x and column y of \mathbf{X} . $\mathbf{I}_{X \times X}$, $\mathbf{0}_{X \times X}$, and $\mathbf{1}_{X \times X}$ denote the $X \times X$ identity, all zero, and all 1 matrices, respectively. $|\cdot|$ is the absolute value operator, $|\mathbf{x}|$ denotes the element-wise absolute value of a vector \mathbf{x} , and $\text{diag}(\mathbf{x})$ is used to denote a diagonal matrix, where the diagonal elements are given by vector \mathbf{x} . $\mathbb{E}_{x,y}[\cdot]$ denotes the expectation over x and y , and $\Re\{\cdot\}$ and $\Im\{\cdot\}$ are the real and imaginary parts of a complex quantity, respectively. $\nabla_{\mathbf{x}}$ and $\Delta_{\mathbf{x}}^2$ represent the first and the second-order partial derivatives operator, i.e., $\nabla_{\mathbf{x}} = [\frac{\partial}{\partial x_1}, \dots, \frac{\partial}{\partial x_N}]^T$ and $\Delta_{\mathbf{x}}^2 = \nabla_{\mathbf{y}} \times \nabla_{\mathbf{x}}^T$. Finally, \otimes denotes circular convolution.

II. SIGNAL MODEL

The complex baseband OFDM signal is given by

$$x_n = \frac{1}{\sqrt{N}} \sum_{k=0}^{N-1} d_k e^{j2\pi kn/N} \quad n = 0, 1, \dots, N-1, \quad (1)$$

where d_k , for $k = 1, \dots, N$, is the modulated pilot symbol, x_n is the n th sample of the transmitted OFDM symbol, N is the number of subcarriers, and k denotes the subcarrier index. At the receiver, the complex baseband received signal, r_n , is given by

$$r_n = e^{j(\theta_n + 2\pi n\epsilon/N)} s_n + w_n, \quad (2)$$

where $s_n \triangleq h_n \otimes x_n$ is the received OFDM training symbol, $\{\theta_n\}_{n=0}^{N-1}$ is the discrete-time PHN sequence, ϵ is the normalized CFO, which is modeled as an *unknown deterministic* parameter [5], $\{h_l\}_{l=0}^{L-1}$ is the channel impulse response and L is the channel length. The channel is assumed to be quasi-static, which is constant and *known* over the OFDM symbol duration and changes from symbol to symbol following a complex Gaussian distribution, i.e., $h_l \sim \mathcal{CN}(\mu_{h_l}, \sigma_{h_l}^2)$. Since the channel, PHN and CFO can be estimated jointly using pilots and the algorithm in [3], this paper focuses on PHN and CFO estimation and proposes ECM based algorithm to improve the algorithm's computational complexity (cf. Section IV-C). In addition, $\{w_n\}_{n=0}^{N-1}$ is the complex *additive white Gaussian noise* (AWGN) with zero-mean and known variance σ_w^2 . The PHN is modeled as a Wiener process, i.e., $\theta_n = \theta_{n-1} + \delta_n$, $\forall n$, where $\delta_n \sim \mathcal{N}(0, \sigma_\delta^2)$ is the PHN innovation and σ_δ^2 is the variance of the innovation process [11],[12]. The received signal, $\mathbf{r} \triangleq [r_0, r_1, \dots, r_{N-1}]^T$, in matrix form is given by

$$\mathbf{r} = \mathbf{E}\mathbf{P}\mathbf{F}^H\mathbf{H}\mathbf{d} + \mathbf{w}, \quad (3)$$

where

- $\mathbf{E} \triangleq \text{diag}([e^{j2\pi\epsilon/N} \times 0, \dots, e^{j2\pi\epsilon/N} \times (N-1)]^T)$,
- $\mathbf{P} \triangleq \text{diag}([e^{j\theta_0}, e^{j\theta_1}, \dots, e^{j\theta_{N-1}}]^T)$,
- \mathbf{F} is an $N \times N$ DFT matrix, i.e., $[\mathbf{F}]_{l,m} \triangleq (1/\sqrt{N})e^{-j(2\pi ml/N)}$ for $m, l = 0, 1, \dots, N-1$,
- $\mathbf{H} \triangleq \text{diag}(\mathbf{h}) = \text{diag}([h_0, h_1, \dots, h_{N-1}]^T)$,
- $\mathbf{d} \triangleq [d_0, d_1, \dots, d_{N-1}]^T$, and
- $\mathbf{w} \triangleq [w_0, \dots, w_{N-1}]^T$.

III. DERIVATION OF THE HYBRID CRAMÉR-RAO BOUND

In this section, the HCRB for joint estimation of PHN and CFO parameters in OFDM systems is derived. Let $\boldsymbol{\lambda} = [\boldsymbol{\theta}^T \epsilon]^T$ be the vector of hybrid parameters of interest, where $\boldsymbol{\theta} \triangleq [\theta_0, \dots, \theta_{N-1}]^T$ is a vector of random PHN parameters and ϵ is the deterministic CFO parameter. The accuracy of estimating $\boldsymbol{\lambda}$ is lower bounded by the HCRB ($\boldsymbol{\Omega}$) as [13]

$$\mathbb{E}_{\mathbf{r}, \boldsymbol{\theta} | \epsilon} \left[(\hat{\boldsymbol{\lambda}}(\mathbf{r}) - \boldsymbol{\lambda})(\hat{\boldsymbol{\lambda}}(\mathbf{r}) - \boldsymbol{\lambda})^T \right] \succeq \boldsymbol{\Omega}. \quad (4)$$

Let us define $\mathbf{B} = \boldsymbol{\Omega}^{-1}$ as the $(N+1) \times (N+1)$ hybrid information matrix (HIM), which can be partitioned as

$$\mathbf{B} = \begin{bmatrix} \mathbf{B}_{11} & \mathbf{b}_{12} \\ \mathbf{b}_{21} & b_{22} \end{bmatrix}, \quad (5)$$

where the $N \times N$ matrix \mathbf{B}_{11} and the scalar b_{22} are the hybrid information matrix and scalar for the estimation of $\boldsymbol{\theta}$ and ϵ , respectively. In addition, \mathbf{b}_{12} and \mathbf{b}_{21} are $N \times 1$ and $1 \times N$ vectors, respectively.

Theorem: The HCRB for joint estimation of PHN and CFO is given by

$$\boldsymbol{\Omega} = \begin{bmatrix} \mathbf{B}_{11}^{-1} + \mathbf{V}_N & -\vartheta^{-1} \mathbf{B}_{11}^{-1} \mathbf{b}_{12} \\ -\vartheta^{-1} \mathbf{b}_{12}^T \mathbf{B}_{11}^{-1} & \vartheta^{-1} \end{bmatrix}, \quad (6)$$

where

- $\vartheta \triangleq \xi_{D4} - \mathbf{b}_{12}^T \mathbf{B}_{11}^{-1} \mathbf{b}_{12}$,
- $\xi_{D4} \triangleq \frac{2}{\sigma_w^2} \mathbf{d}^H \mathbf{H}^H \mathbf{F} \mathbf{M} \mathbf{F}^H \mathbf{H} \mathbf{d}$,
- $\mathbf{V}_N \triangleq \vartheta^{-1} \mathbf{B}_{11}^{-1} \mathbf{b}_{12} \mathbf{b}_{12}^T \mathbf{B}_{11}^{-1}$,
- $\mathbf{b}_{12} = \mathbf{b}_{21}^T = \frac{2}{\sigma_w^2} \mathbf{d}^H \mathbf{H}^H \mathbf{F} \sqrt{\mathbf{M}} \mathbf{U}_n \mathbf{F}^H \mathbf{H} \mathbf{d}$,
- $\mathbf{B}_{11} = \boldsymbol{\Xi}_{D1} + \boldsymbol{\Xi}_{P1}$,
- $[\boldsymbol{\Xi}_{D1}]_{n,n} = \frac{2}{\sigma_w^2} \mathbf{d}^H \mathbf{H}^H \mathbf{F} \mathbf{U}_n \mathbf{F}^H \mathbf{H} \mathbf{d}$, and $\boldsymbol{\Xi}_{P1}$ is defined in Appendix A.

Proof: See Appendix A.

IV. PROPOSED ECM BASED ESTIMATOR

In this section, an ECM based algorithm for joint estimation of the PHN and CFO is derived. Fig.1 shows the proposed ECM estimator. As shown in this figure, the algorithm iterates between the expectation step (E-step) and the maximization step (M-step). In E-step, Kalman filter is proposed to estimate the PHN vector $\boldsymbol{\theta}^{[i]}$, using the CFO estimate $\hat{\epsilon}^{[i]}$ obtained from the previous (i th) iteration, while in M-step, a closed-form estimator is applied to update the CFO estimate $\hat{\epsilon}^{[i+1]}$. The proposed ECM algorithm at the i th iteration as follows. For

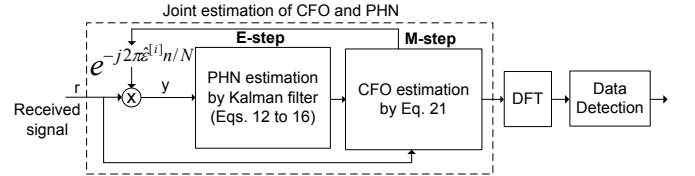


Fig. 1. Proposed estimator based on an ECM algorithm

the given problem, let the received data \mathbf{r} be and incomplete data. The complete data is defined as $\mathbf{z} \triangleq [\mathbf{r}^T \boldsymbol{\theta}^T]^T$ [5]. The log likelihood function of the complete data, $\log p(\mathbf{z}; \epsilon)$, is given by

$$\log p(\mathbf{z}; \epsilon) = \text{C1} + \frac{1}{\sigma_w^2} \sum_{n=0}^{N-1} \| r_n - e^{j2\pi n\epsilon/N} e^{j\theta_n} s_n \|^2 + \log p(\theta_0) + \sum_{n=0}^{N-1} \log p(\theta_n | \theta_{n-1}), \quad (7)$$

where C1 is a constant. The detailed E-step and M-step for estimating the CFO and PHN are as follows:

E-step: In this step, the received signal r_n is first multiplied by $e^{-j2\pi\hat{\epsilon}^{[i]}/N}$, then the signal y_n is used to estimate the PHN vector, where $\hat{\epsilon}^{[i]}$ is the latest CFO estimate obtained from the previous iteration. We proposed to use extended Kalman filter (EKF) during E-step to estimate the PHN samples $\boldsymbol{\theta}$. The PHN estimation is as follows: The signal y_n can be written as

$$y_n = e^{-j2\pi n\hat{\epsilon}^{[i]}/N} r_n = e^{j2\pi n\Delta\epsilon/N} e^{j\theta_n} s_n + \tilde{w}_n, \quad (8)$$

where $\Delta\epsilon \triangleq \epsilon - \hat{\epsilon}^{[i]}$ and $\tilde{w}_n \triangleq w_n e^{-j2\pi n \hat{\epsilon}^{[i]}/N}$. The state and observation equations at time n are given by

$$\theta_n = \theta_{n-1} + \delta_n, \quad (9)$$

$$y_n = z_n + w_n = e^{j2\pi n \Delta\epsilon/N} e^{j\theta_n} s_n + \tilde{w}_n. \quad (10)$$

Since the observation equation in (10) is a non-linear function of the unknown state vector θ , the EKF is used instead. The EKF uses Taylor series expansion to linearize the non-linear observation equation in (10) about the current estimates [14]. Thus, the Jacobian of z_n is evaluated by computing the first order partial derivative of z_n with respect to θ_n as

$$\begin{aligned} \dot{z}_n &= \frac{\partial z(\Delta\hat{\epsilon}^{[i]}, \theta_n)}{\partial \theta_n} \Big|_{\theta_n = \hat{\theta}_{n|n-1}} = jz(\Delta\hat{\epsilon}^{[i]}, \hat{\theta}_{n|n-1}) \quad (11) \\ &= j e^{j2\pi n \Delta\hat{\epsilon}^{[i]}/N} e^{j\hat{\theta}_{n|n-1}} s_n, \end{aligned}$$

where \dot{z} denotes the Jacobian of z evaluated at θ_n . The first and second moments of the state vector at the i th iteration denoted by $\hat{\theta}_{n|n-1}^{[i]}$ and $\mathbf{M}_{n|n-1}^{[i]}$, respectively, are given by

$$\hat{\theta}_{n|n-1}^{[i]} = \hat{\theta}_{n-1|n-1}^{[i]}, \quad (12)$$

$$\mathbf{M}_{n|n-1}^{[i]} = \mathbf{M}_{n-1|n-1}^{[i]} + \sigma_\delta^2, \quad (13)$$

Given the observation y_n , the Kalman gain \mathbf{K}_n , posteriori state estimate $\hat{\theta}_{n|n}^{[i]}$, and the filtering error covariance, $\mathbf{M}_{n|n}^{[i]}$ are given by

$$\begin{aligned} \mathbf{K}_n &= \mathbf{M}_{n|n-1}^{[i]} \dot{z}^*(\hat{\epsilon}^{[i]}, \theta_{n|n-1}) (\dot{z}(\Delta\hat{\epsilon}^{[i]}, \theta_{n|n-1}) \mathbf{M}_{n-1|n-1}^{[i]} \\ &\quad \times \dot{z}^*(\hat{\epsilon}^{[i]}, \theta_{n|n-1}) + \sigma_w^2)^{-1}, \quad (14) \end{aligned}$$

$$\hat{\theta}_{n|n}^{[i]} = \hat{\theta}_{n|n-1}^{[i]} + \Re\{\mathbf{K}_n (y_n - e^{j2\pi n \Delta\hat{\epsilon}^{[i]}/N} e^{j\hat{\theta}_{n|n-1}^{[i]}} s_n)\}, \quad (15)$$

$$\mathbf{M}_{n|n}^{[i]} = \Re\{\mathbf{M}_{n|n-1}^{[i]} - \mathbf{K}_n \dot{z}(\Delta\hat{\epsilon}^{[i]}, \theta_{n|n-1}) \mathbf{M}_{n|n-1}^{[i]}\}, \quad (16)$$

Before starting the EKF recursion (11)-(16), $\hat{\theta}_{1|0}^{[0]}$ and $\mathbf{M}_{1|0}^{[0]}$ are initialized by $\hat{\theta}_{1|0}^{[0]} = 0$ and $\mathbf{M}_{1|0}^{[0]} = \sigma_\delta^2$.

M-step: By minimizing the likelihood function in (7), the CFO estimate update, $\hat{\epsilon}^{[i+1]}$, in M-step is given by

$$\hat{\epsilon}^{[i+1]} = \arg \min_{\epsilon} \sum_{n=0}^{N-1} \| r_n - e^{j2\pi n \epsilon/N} e^{j\theta_n} s_n \|^2 \Big|_{\theta_n = \hat{\theta}_n^{[i]}} \quad (17)$$

After simplifying (17), we have

$$\hat{\epsilon}^{[i+1]} = \arg \max_{\epsilon} \sum_{n=0}^{N-1} \Re\{(r_n)^* S_n^{[i]} e^{j2\pi n \epsilon/N}\} \quad (18)$$

where $S_n^{[i]} = e^{j\theta_n^{[i]}} s_n$. The Taylor series expansion of $e^{j2\pi n \epsilon/N}$ around the previous CFO estimate, $\hat{\epsilon}^{[i]}$, up to the second order term is given by

$$\begin{aligned} e^{j2\pi n \epsilon/N} &= e^{j2\pi n \hat{\epsilon}^{[i]}/N} + (\epsilon - \hat{\epsilon}^{[i]}) (j \frac{2\pi}{N} n) e^{j2\pi n \hat{\epsilon}^{[i]}/N} \\ &\quad + \frac{1}{2} (\epsilon - \hat{\epsilon}^{[i]})^2 (j \frac{2\pi}{N} n)^2 e^{j2\pi n \hat{\epsilon}^{[i]}/N} \quad (19) \end{aligned}$$

Substituting (19) into (18), $\hat{\epsilon}^{[i+1]}$ is given by

$$\begin{aligned} \hat{\epsilon}^{[i+1]} &= \arg \max_{\epsilon} \left\{ \sum_{n=0}^{N-1} \Re\{(r_n)^* S_n^{[i]} e^{j2\pi n \hat{\epsilon}^{[i]}/N}\} \right. \\ &\quad \left. + (\epsilon - \hat{\epsilon}^{[i]}) \sum_{n=0}^{N-1} \Re\{(r_n)^* S_n^{[i]} (j \frac{2\pi}{N} n) e^{j2\pi n \hat{\epsilon}^{[i]}/N}\} \right. \\ &\quad \left. + \frac{1}{2} (\epsilon - \hat{\epsilon}^{[i]})^2 \sum_{n=0}^{N-1} \Re\{(r_n)^* S_n^{[i]} (j \frac{2\pi}{N} n)^2 e^{j2\pi n \hat{\epsilon}^{[i]}/N}\} \right\} \quad (20) \end{aligned}$$

Taking the derivative of (20) with respect to ϵ and equating the result to zero, the estimate of ϵ at the $(i+1)$ th iteration is given by:

$$\hat{\epsilon}^{[i+1]} = \hat{\epsilon}^{[i]} + \frac{N \sum_{n=0}^{N-1} n \Im\{(r_n)^* S_n^{[i]} e^{j2\pi n \hat{\epsilon}^{[i]}/N}\}}{2\pi \sum_{n=0}^{N-1} n^2 \Re\{(r_n)^* S_n^{[i]} e^{j2\pi n \hat{\epsilon}^{[i]}/N}\}}, \quad (21)$$

Using (15) and (21), the proposed algorithm iteratively updates the PHN and CFO estimates in E-step and M-step of the algorithm, respectively, and stops when the difference between likelihood functions of two iterations is smaller than a threshold ζ , i.e.,

$$\begin{aligned} &\left| \sum_{n=0}^{N-1} \left\| r_n - e^{j2\pi n \hat{\epsilon}^{[i+1]}/N} e^{j\hat{\theta}_n^{[i+1]}} s_n \right\|^2 \right. \\ &\quad \left. - \sum_{n=0}^{N-1} \left\| r_n - e^{j2\pi n \hat{\epsilon}^{[i]}/N} e^{j\hat{\theta}_n^{[i]}} s_n \right\|^2 \right| \leq \zeta. \quad (22) \end{aligned}$$

It has been found through simulations that: 1) The appropriate initialization of CFO, i.e., $\hat{\epsilon}^{[0]}$ can help the proposed estimator to estimate the CFO and PHN parameters. The initial estimate of CFO may be obtained using alternating projection via likelihood function, $\sum_{n=0}^{N-1} \| r_n - e^{j2\pi n \hat{\epsilon}/N} s_n \|^2$ using a coarse step size 10^{-2} . 2) The proposed estimator always converges to true estimates. For example, at $SNR = 20$ dB the estimator stops only after 2 iterations, on average. This demonstrates the efficiency of our proposed estimator compared to [4], which require 150 iterations for convergence.

A. Complexity of the proposed estimators

In this section, the computational complexity of the proposed estimator and the algorithm in [3] are compared against one another based on CPU execution time [15]. The execution time is observed at an SNR of 20 dB while using an Intel Core 7 Quad 3.4 GHz processor with 8 GB of RAM. The execution time for the proposed estimator and the algorithm in [3] are determined to be 0.0025 and 1.498 seconds, respectively. These results show that compared to the approach in [3], the proposed estimator is capable of estimating the desired parameters approximately 600 times quicker.

V. SIMULATION RESULTS AND DISCUSSIONS

In this section, the performance of the proposed estimator is compared with the HCRB and MAP estimator. A Rayleigh multipath fading channel with a delay of $L = 4$ taps and an exponentially decreasing power delay profile is assumed. A training symbol size of $N = 64$ subcarriers is used, where subcarrier are modulated using binary phase-shift keying (BPSK)

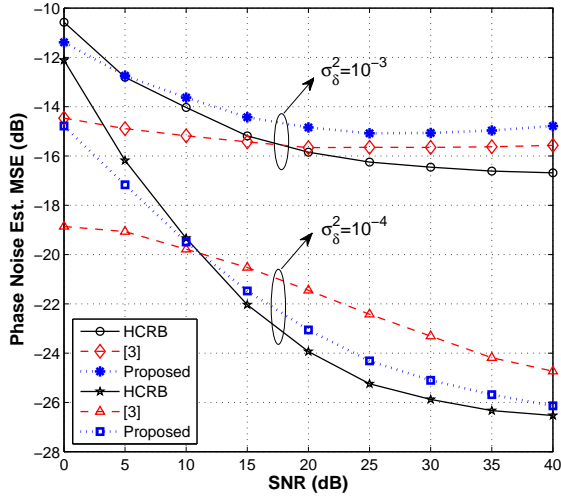


Fig. 2. MSE for the proposed and MAP estimators for phase noise variance, $\sigma_\phi^2 = [10^{-3}, 10^{-4}] \text{ rad}^2$.

scheme. The Wiener PHN is generated with different PHN variances, e.g. $\sigma_\phi^2 = [10^{-3}, 10^{-4}] \text{ rad}^2$. For each simulation, the CFO is randomly picked from the range $\epsilon \in (-0.5, 0.5)$.

Figs. 2 and 3 plot the HCRB and MSE for estimating PHN and CFO, respectively, using both the proposed and MAP estimation algorithms versus SNR. The results lead to the following observations: 1) The HCRB and the proposed estimator's MSE are dependent on the variance of the PHN process and are lower for a lower PHN variance. 2) Figs. 2 and 3 show that CFO and PHN estimation performances suffer from an error floor, which is directly related to the variance of the PHN process. This follows from the fact that at low SNR the performance of the system is dominated by AWGN, while at high SNR the performance of the proposed estimator is limited by PHN and the resulting ICI. 3) It can be clearly observed that the proposed estimator outperforms the algorithms in [3] at moderate PHN variances, e.g., $\sigma_\phi^2 = 10^{-4} \text{ rad}^2$. This performance improvement can be attributed to the fact that the proposed joint PHN and CFO estimator does not apply a small angle approximation to obtain the CFO estimates unlike the approach in [3]. However, for large PHN variances, e.g., $\sigma_\phi^2 = 10^{-3} \text{ rad}^2$, we note that the proposed estimator is slightly outperformed by the approach in [3]. This can be attributed to the sensitivity of the proposed ECM estimator to the initial PHN values, whereas the PHN variance increases the initialization error also increases. Consequently, the proposed estimator's performance degrades slightly. 4) The MSE of the proposed estimator and the approach in [16] are lower than the HCRB at lower SNR. This is due to the fact that the HCRB cannot be derived in closed-form while taking into account the range of CFO values, i.e., $(-0.5, 0.5)$. Thus, the HCRB is higher than the MSE of the proposed estimator at lower SNR.

VI. CONCLUSION

This paper derives a new expression for the HCRB for joint estimation of CFO and PHN. A new iterative estimator that jointly estimates CFO and PHN parameters in OFDM

Note that a similar estimator is also used in [16].

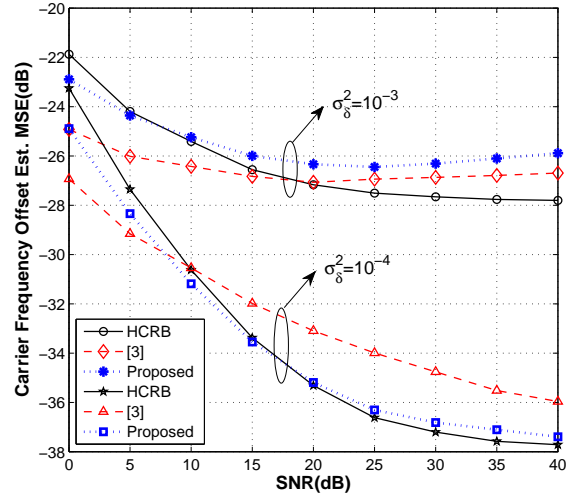


Fig. 3. MSE for the proposed and MAP estimators for phase noise variance, $\sigma_\phi^2 = [10^{-3}, 10^{-4}] \text{ rad}^2$.

systems has been proposed. The proposed estimator is shown to be computationally less complex to implement than existing algorithms while outperforming existing algorithms for moderate PHN variances. Simulation results show on average a 10 dB estimation performance gain compared to the algorithm in [3], [16]. More importantly, simulations indicate that the performance of the proposed estimator is close to the BCRB at moderate to high SNRs.

APPENDIX A DERIVATION OF THE HCRB

The HIM \mathbf{B} can be written as [13]

$$\mathbf{B} = \Xi_D + \Xi_P, \quad (\text{A.1})$$

where $\Xi_D \triangleq \mathbb{E}_\theta [\Psi(\theta, \epsilon)]$ with $\Psi(\theta, \epsilon) \triangleq \mathbb{E}_{\mathbf{r}|\theta, \epsilon} [-\Delta_\lambda^\lambda \log p(\mathbf{r}|\theta, \epsilon)|\epsilon]$ denoting the Fisher's information matrix (FIM) and $\Xi_P \triangleq \mathbb{E}_{\theta|\epsilon} [-\Delta_\lambda^\lambda \log p(\theta|\epsilon)|\epsilon]$ is the prior information matrix with $p(\theta|\epsilon)$ denoting the prior distribution of PHN vector given the CFO. Thus, in this section we first obtain an expression for matrices Ξ_D and Ξ_P

A. Computation of $\Xi_D \triangleq \mathbb{E}_\theta [\Psi(\theta, \epsilon)]$

We partition the matrix $\Psi(\theta, \epsilon)$ as

$$\Psi(\theta, \epsilon) = \begin{bmatrix} \Psi_{11}(\theta, \epsilon) & \psi_{12}(\theta, \epsilon) \\ \psi_{21}(\theta, \epsilon) & \psi_{22}(\theta, \epsilon) \end{bmatrix}, \quad (\text{A.2})$$

where

$$\Psi_{11}(\theta, \epsilon) \triangleq \mathbb{E}_{\mathbf{r}|\theta, \epsilon} [-\Delta_\theta^\theta \log p(\mathbf{r}|\theta, \epsilon)|\epsilon], \quad (\text{A.3})$$

$$\psi_{12}(\theta, \epsilon) \triangleq \mathbb{E}_{\mathbf{r}|\theta, \epsilon} [-\Delta_\epsilon^\theta \log p(\mathbf{r}|\theta, \epsilon)|\epsilon], \quad (\text{A.4})$$

$$\psi_{21}(\theta, \epsilon) \triangleq \mathbb{E}_{\mathbf{r}|\theta, \epsilon} [-\Delta_\theta^\epsilon \log p(\mathbf{r}|\theta, \epsilon)|\epsilon], \quad (\text{A.5})$$

$$\psi_{22}(\theta, \epsilon) \triangleq \mathbb{E}_{\mathbf{r}|\theta, \epsilon} [-\Delta_\epsilon^\epsilon \log p(\mathbf{r}|\theta, \epsilon)|\epsilon]. \quad (\text{A.6})$$

1) Computation of $\Xi_{D1} \triangleq \mathbb{E}_\theta [\Psi_{11}(\theta, \epsilon)]$: To compute the log-likelihood function in (A.3), $p(\mathbf{r}|\theta, \epsilon)$ is given by

$$p(\mathbf{r}|\theta, \epsilon) = C \exp \left[\frac{-1}{\sigma_w^2} (\mathbf{r} - \boldsymbol{\mu}(\epsilon))^H (\mathbf{r} - \boldsymbol{\mu}(\epsilon)) \right], \quad (\text{A.7})$$

where $C \triangleq (\pi \sigma_w^2)^{-N}$ and given θ and ϵ , \mathbf{r} is a complex Gaussian vector with mean vector $\boldsymbol{\mu}(\epsilon) = \mathbf{E} \mathbf{P} \mathbf{F}^H \mathbf{H} \mathbf{d}$ and covariance matrix $\sigma_w^2 \mathbf{I}_N$. Based on (A.7), it follows that:

$$-\Delta_{\theta}^{\theta} \log p(\mathbf{r}|\boldsymbol{\theta}, \epsilon) = \frac{1}{\sigma_w^2} \left(-\mathbf{r}^H \Delta_{\theta}^{\theta}(\boldsymbol{\mu}(\epsilon)) - \Delta_{\theta}^{\theta}(\boldsymbol{\mu}^H(\epsilon))\mathbf{r} + \Delta_{\theta}^{\theta}(\boldsymbol{\mu}^H(\epsilon)\boldsymbol{\mu}(\epsilon)) \right). \quad (\text{A.8})$$

The expected value of (A.8) with respect to \mathbf{r} is given by

$$\mathbb{E}_{\mathbf{r}|\boldsymbol{\theta}, \epsilon}[-\Delta_{\theta}^{\theta} \log p(\mathbf{r}|\boldsymbol{\theta}, \epsilon)] = \frac{1}{\sigma_w^2} \left(-\boldsymbol{\mu}^H(\epsilon) \Delta_{\theta}^{\theta}(\boldsymbol{\mu}(\epsilon)) - \Delta_{\theta}^{\theta}(\boldsymbol{\mu}^H(\epsilon))\boldsymbol{\mu}(\epsilon) + \Delta_{\theta}^{\theta}(\boldsymbol{\mu}^H(\epsilon)\boldsymbol{\mu}(\epsilon)) \right). \quad (\text{A.9})$$

Using $\Delta_{\theta}^{\theta}(\boldsymbol{\mu}^H(\epsilon)\boldsymbol{\mu}(\epsilon)) = \Delta_{\theta}^{\theta}(\boldsymbol{\mu}^H(\epsilon))\boldsymbol{\mu}(\epsilon) + \boldsymbol{\mu}^H(\epsilon)\Delta_{\theta}^{\theta}(\boldsymbol{\mu}^H(\epsilon)) + 2\nabla_{\theta}(\boldsymbol{\mu}(\epsilon))\nabla_{\theta}(\boldsymbol{\mu}^H(\epsilon))$, Ξ_{D1} is found to be an $N \times N$ diagonal matrix, such that

$$[\Xi_{D1}]_{n,n} = \frac{2}{\sigma_w^2} \mathbf{d}^H \mathbf{H}^H \mathbf{F} \mathbf{U}_n \mathbf{F}^H \mathbf{H} \mathbf{d}. \quad (\text{A.10})$$

where $\mathbf{U}_n \triangleq \text{diag}([\mathbf{0}_{1 \times (n-1)}, 1, \mathbf{0}_{1 \times (N-n)}])$.

2) *Computation of $\xi_{D4} = \mathbb{E}_{\boldsymbol{\theta}}[\psi_{22}(\boldsymbol{\theta}, \epsilon)]$, $\xi_{D3} = \mathbb{E}_{\boldsymbol{\theta}}[\psi_{21}(\boldsymbol{\theta}, \epsilon)]$ and $\xi_{D2} = \mathbb{E}_{\boldsymbol{\theta}}[\psi_{12}(\boldsymbol{\theta}, \epsilon)]$* : Based on (A.7), it follows that:

$$-\Delta_{\epsilon}^{\epsilon} \log p(\mathbf{r}|\boldsymbol{\theta}, \epsilon) = \frac{1}{\sigma_w^2} \left(-\mathbf{r}^H \Delta_{\epsilon}^{\epsilon}(\boldsymbol{\mu}(\epsilon)) - \Delta_{\epsilon}^{\epsilon}(\boldsymbol{\mu}^H(\epsilon))\mathbf{r} + \Delta_{\epsilon}^{\epsilon}(\boldsymbol{\mu}^H(\epsilon)\boldsymbol{\mu}(\epsilon)) \right) \quad (\text{A.11})$$

The expected value of (A.11) with respect to \mathbf{r} is given by

$$\mathbb{E}_{\mathbf{r}|\boldsymbol{\theta}, \epsilon}[-\Delta_{\epsilon}^{\epsilon} \log p(\mathbf{r}|\boldsymbol{\theta}, \epsilon)] = \frac{1}{\sigma_w^2} \left(-\boldsymbol{\mu}^H \Delta_{\epsilon}^{\epsilon}(\boldsymbol{\mu}(\epsilon)) - \Delta_{\epsilon}^{\epsilon}(\boldsymbol{\mu}^H(\epsilon))\boldsymbol{\mu} + \Delta_{\epsilon}^{\epsilon}(\boldsymbol{\mu}^H(\epsilon)\boldsymbol{\mu}(\epsilon)) \right). \quad (\text{A.12})$$

By following the simplification given above (A.10), we obtain

$$\xi_{D4} \triangleq \mathbb{E}_{\boldsymbol{\theta}}[\Psi_{22}(\boldsymbol{\theta}, \epsilon)] = \frac{2}{\sigma_w^2} \mathbf{d}^H \mathbf{H}^H \mathbf{F} \mathbf{M} \mathbf{F}^H \mathbf{H} \mathbf{d}, \quad (\text{A.13})$$

where $\mathbf{M} \triangleq \text{diag} \left([(2\pi \frac{0}{N})^2, (2\pi \frac{1}{N})^2, \dots, (2\pi \frac{N-1}{N})^2]^T \right)$. Moreover, by following similar steps as in (A.8)-(A.13), it can be found that $\xi_{D2} \triangleq \mathbb{E}_{\boldsymbol{\theta}}[\Psi_{12}(\boldsymbol{\theta}, \epsilon)]$ is an $N \times 1$ vector with n th element given by

$$[\xi_{D2}]_{n,1} = \frac{2}{\sigma_w^2} \left[\mathbf{d}^H \mathbf{H}^H \mathbf{F} \sqrt{\mathbf{M}} \mathbf{U}_n \mathbf{F}^H \mathbf{H} \mathbf{d} \right], \quad (\text{A.14})$$

Finally, ξ_{D3} can be determined as $\xi_{D3} = \xi_{D2}^T$.

B. Computation of $\Xi_P \triangleq \mathbb{E}_{\boldsymbol{\theta}|\epsilon}[-\Delta_{\lambda}^{\lambda} \log p(\boldsymbol{\theta}|\epsilon)|\epsilon]$

The second factor in HIM, defined in (A.1), can be written as:

$$\mathbb{E}_{\boldsymbol{\theta}|\epsilon}[-\Delta_{\lambda}^{\lambda} \log p(\boldsymbol{\theta}|\epsilon)|\epsilon] \triangleq \begin{bmatrix} \Xi_{P1} & \xi_{P2} \\ \xi_{P3} & \xi_{P4} \end{bmatrix} = \begin{bmatrix} \mathbb{E}_{\boldsymbol{\theta}}[-\Delta_{\theta}^{\theta} \log p(\boldsymbol{\theta})] & \mathbb{E}_{\boldsymbol{\theta}}[-\Delta_{\epsilon}^{\epsilon} \log p(\boldsymbol{\theta})] \\ \mathbb{E}_{\boldsymbol{\theta}}[-\Delta_{\theta}^{\theta} \log p(\boldsymbol{\theta})]^T & \mathbb{E}_{\boldsymbol{\theta}}[-\Delta_{\epsilon}^{\epsilon} \log p(\boldsymbol{\theta})] \end{bmatrix}. \quad (\text{A.15})$$

where $p(\boldsymbol{\theta})$ is the prior distribution of $\boldsymbol{\theta}$.

1) *Computation of $\Xi_{P1} \triangleq \mathbb{E}_{\boldsymbol{\theta}}[-\Delta_{\theta}^{\theta} \log p(\boldsymbol{\theta})]$* : From [17, eq.(19)], we obtain the $N \times N$ matrix $\mathbb{E}_{\boldsymbol{\theta}}[-\Delta_{\theta}^{\theta} \log p(\boldsymbol{\theta})]$ as

$$\Xi_{P1} = \frac{-1}{\sigma_{\delta}^2} \begin{bmatrix} -1 & 1 & 0 & \cdots & 0 \\ 1 & -2 & 1 & 0 & \vdots \\ 0 & \ddots & \ddots & \ddots & 0 \\ \vdots & 0 & 1 & -2 & 1 \\ 0 & \cdots & 0 & 1 & -1 \end{bmatrix} \quad (\text{A.16})$$

2) *Computation of $\xi_{P2} \triangleq \mathbb{E}_{\boldsymbol{\theta}}[-\Delta_{\theta}^{\epsilon} \log p(\boldsymbol{\theta})]$ and $\xi_{P4} \triangleq \mathbb{E}_{\boldsymbol{\theta}}[-\Delta_{\epsilon}^{\epsilon} \log p(\boldsymbol{\theta})]$* : Since CFO is a deterministic parameter, we have

$$\xi_{P2} = \xi_{P3}^T = \mathbf{0}_{N \times 1}, \quad (\text{A.17})$$

$$\xi_{P4} = 0. \quad (\text{A.18})$$

Using the above results, we can evaluate the HIM in (5), since $\mathbf{B}_{11} = \xi_{D1} + \xi_{P1}$, $\mathbf{b}_{12} = \mathbf{b}_{21}^T = \xi_{D2} + \xi_{P2} = \xi_{D2}$, and $\mathbf{b}_{22} = \xi_{D4}$.

Using the HIM, the block-matrix inversion in [14] can be used to find the inverse of the HIM or the HCRB as shown in (6).

REFERENCES

- [1] Y. Zhang and H.-H. Chen, *Mobile wimax: toward broadband wireless metropolitan area networks*. New York, USA: Taylor & Francis Group, 2008.
- [2] A. Garcia Armada, "Understanding the effects of phase noise in orthogonal frequency division multiplexing (OFDM)," *IEEE Trans. Broadcast.*, vol. 47, no. 2, pp. 153–159, Jun 2001.
- [3] D. D. Lin, R. Pacheco, T. J. Lim, and D. Hatzinakos, "Joint estimation of channel response, frequency offset, and phase noise in OFDM," *IEEE Trans. Signal Process.*, vol. 54, no. 9, pp. 3542–3554, Sept. 2006.
- [4] R. Carvajal, J. C. Aguero, B. I. Godoy, and G. C. Goodwin, "EM-based maximum-likelihood channel estimation in multicarrier systems with phase distortion," *IEEE Trans. Veh. Technol.*, vol. 62, no. 1, pp. 152–160, Jan. 2013.
- [5] E. P. Simon, L. Ros, H. Hijazi, and M. Ghogho, "Joint carrier frequency offset and channel estimation for OFDM systems via the EM algorithm in the presence of very high mobility," *IEEE Trans. Signal Process.*, vol. 60, no. 2, pp. 754–765, Feb. 2012.
- [6] J. Yang, B. Geller, , and A. Wei, "Bayesian and hybrid cramer-rao bounds for qam dynamical phase estimation," in *Proc. Acoustics, Speech and Signal Processing ICASSP*, Taipei, Taiwan, Apr 2009, pp. 3297–3300.
- [7] J. Yang, B. Geller, and S. Bay, "Bayesian and hybrid cramer-rao bounds for the carrier recovery under dynamic phase uncertain channels," *IEEE Trans. Signal Process.*, vol. 59, no. 2, pp. 667–680, Feb. 2011.
- [8] H. Hijazi, L. Fawaz, A. Akra, and E. Simon, "Hybrid cramer-rao bound for dynamical time-varying channel and carrier frequency offset estimation in ofdm systems," in *Proc. 19th International Conference on Telecommunications (ICT)*, Jounieh / Lebanon, april 2012.
- [9] S. Bay, B. Geller, A. Renaux, J. Barbot, and J. Brossier, "On the hybrid Cramér-Rao bound and its application to dynamical phase estimation," *IEEE Signal Process. Lett.*, vol. 15, pp. 453–456, 2008.
- [10] A. A. Nasir, H. Mehrpouyan, R. Schober, and Y. Hua, "Phase noise in MIMO systems: Bayesian Cramér-Rao bounds and soft-input estimation," *IEEE Trans. Signal Process.*, in press.
- [11] A. M. A. Demir and J. Roychowdhury, "Phase noise in oscillators: A unifying theory and numerical methods for characterization," *IEEE Trans. Biomed. Circuits Syst.*, vol. 47, pp. 655–674, May 2000.
- [12] D. Lin, R. Pacheco, T. J. Lim, and D. Hatzinakos, "Optimal OFDM channel estimation with carrier frequency offset and phase noise," in *Proc. IEEE (WCNC)*, Apr 2006.
- [13] H. L. van Trees and K. L. Bell, *Bayesian bounds for parameter estimation and nonlinear filtering/tracking*. New York, USA: John Wiley and Sons, 2007.
- [14] S. M. Kay, *Fundamentals of Statistical Signal Processing, Estimation Theory*. Signal Processing Series: Prentice Hall, 1993.
- [15] N. Moller, "On schoonhages algorithm and subquadratic integer gcd computation," *Mathematics of Computation*, vol. 77, pp. 589–607, Jan. 2008.
- [16] D. D. Lin and T. J. Lim, "The variational inference approach to joint data detection and phase noise estimation in ofdm," *IEEE Trans. Signal Process.*, vol. 55, no. 5, pp. 1862–1874, May 2007.
- [17] S. Bay, C. Herzet, J.-M. Brossier, J.-P. Barbot, and B. Geller, "Analytic and Asymptotic Analysis of Bayesian Cramér-Rao Bound for Dynamical Phase Offset Estimation," *IEEE Trans. Signal Process.*, vol. 56, no. 1, pp. 61–70, Jan. 2008.